

RESEARCH

Open Access



# Investigation of a new modulated aperture using speckle techniques

A. M. Hamed\*

## Abstract

**Background:** A design of equally spaced eight-circles placed at equal distances from the origin is suggested. Three models corresponding to the eight-circle design considering conic, linear, and quadratic distributions are investigated. This arrangement is considered for the sake of improving both microscope resolution and image contrast as compared with the pure annular aperture. This design is different compared with other recent work on aperture modulation.

**Results and discussions:** The point spread function (PSF) is computed in all the models using the fast Fourier transform (FFT) algorithm that computes the discrete Fourier transform (DFT) corresponding to the models and compared with the corresponding PSF in the case of uniform circular aperture. In addition, the autocorrelation images for the apertures are shown differently. It is shown smooth pattern for the circular arrangement as compared with the deformation and shrinking appeared in the central peak in case of conic model. Finally, the speckle images corresponding to the considered apertures are investigated. Reconstructed apertures are obtained from the speckle images using the FFT algorithm.

**Conclusions:** The PSF is computed for the described models, and the autocorrelation corresponding to the apertures showed difference. The reconstructed apertures from the speckle images can be improved using filtering techniques. It is noted that MATLAB codes are constructed in the computations of all images and plots.

**Keywords:** Modulated apertures, Point spread function, Speckle imaging

## 1 Background

The speckle effect [1–5] is a result of the interference of many waves of the same frequency, having different phases and amplitudes, which add together to give a resultant wave whose amplitude, and therefore, intensity varies randomly. The size of the speckles is a function of the wavelength of the light, the size of the laser beam which illuminates the first surface, and the distance between this surface and the plane where the speckle pattern is formed. Dainty [3] derives an expression for the mean speckle size as  $\sigma = \lambda z/D$  where  $D$  is the width of the illuminated area, and  $z$  is the distance between the object and the location of the speckle pattern.

A multiple-image encryption based on different modulated apertures in an optical set-up under a holographic arrangement was proposed in [6]. The system is a security architecture that uses different pupil aperture mask in the encoding lens to encrypt different images. The technique is based on multiplexing to perform high-density holographic storage [7].

Speckle can be modeled by analysis of the statistics of the image of a phase object such as a rough surface. The image can be calculated using the coherent transfer function of the imaging system and the angular spectrum representation. This approach gives a three-dimensional image and includes the effects of high numerical aperture and the finite depth of the structure. Different correlation coefficients can be assumed, including fractal distributions, such as exponential correlation, as well as Gaussian correlation [8]. The laser speckle contrast images (LSCI)

\*Correspondence: amhamed73@hotmail.com  
Physics Department, Faculty of Sciences, Ain Shams University,  
Cairo 11566, Egypt

are investigated in many biomedical publications [9–19] while using modulated apertures as in [20].

Linear and quadratic apertures are used in the formation of speckle images [21, 22]. While annular Hermite Gaussian aperture is investigated in [23].

Recently, a slab waveguide that comprises a linear substrate, an exponential graded index guiding layer, and a power-dependent refractive index covering medium is investigated [24]. While a three-layer slab waveguide with a graded index film and a nonlinear substrate is shown [25]. In addition, other work of a planar waveguide with an exponential grade-index guiding layer and a nonlinear cladding is given in [26]. A numerical analysis is presented in [27] for the proposal of a novel decahedron photonic crystal fiber where the central elliptic core is filled with a highly nonlinear 2D material molybdenum disulphide ( $\text{MoS}_2$ ).

In this paper, we designed a new aperture, composed of eight equally spaced conic circles placed shifted outside the center and using it in the formation of speckle image. Reconstruction of the aperture is obtained. In addition, we computed the PSF and the autocorrelation corresponding to the cited model. The aim of the work using the cited apertures is to gain better transverse resolution and improved contrast as compared with annular apertures that gives poorer contrast.

## 2 Methods

A new aperture, in the form of eight equally spaced conic circles and placed at a constant distance from the center, is fabricated. Where four circles are placed along the cartesian coordinates while the other four circles placed along the rotated coordinates by angle  $= 45^\circ$ . The design of this aperture and other similar arrangements using the linear and the quadratic distributions is realized using MATLAB code. In the next, theoretical analysis corresponding to the design of the conic arrangement of eight conic circles is given followed by the computation of the PSF using the FFT algorithm.

### 2.1 Theoretical analysis

The equally spaced eight conic apertures shown in Fig. 1 is described as follows:

$$P_T(x, y) = P_1 + P_2 + \dots + P_8 \quad (1)$$

with the apertures  $P_{1,2}$  located along the  $x$ -axis at distances  $\pm x_0$ , and the apertures  $P_{3,4}$  located along the  $y$ -axis at distances  $\pm y_0$  represented as follows:

$$P_{1,2}(x, y) = 1 - \sqrt{(x \pm x_0)^2 + y^2} \quad (2)$$

$$P_{3,4}(x, y) = 1 - \sqrt{x^2 + (y \pm y_0)^2} \quad (3)$$

For rotated coordinates by angle  $45^\circ$ , another four apertures are shown in the same Fig. 1 and represented as follows:

$$P_{5,6}(x, y) = 1 - \sqrt{\left(x \pm \frac{x_0}{\sqrt{2}}\right)^2 + \left(y \pm \frac{y_0}{\sqrt{2}}\right)^2} \quad (4)$$

$$P_7(x, y) = 1 - \sqrt{\left(x - \frac{x_0}{\sqrt{2}}\right)^2 + \left(y + \frac{y_0}{\sqrt{2}}\right)^2} \quad (5)$$

$$P_8(x, y) = 1 - \sqrt{\left(x + \frac{x_0}{\sqrt{2}}\right)^2 + \left(y - \frac{y_0}{\sqrt{2}}\right)^2} \quad (6)$$

The Fourier transform corresponding to this model of eight conic apertures is not easily solved while we make use of the FFT technique to solve it getting the PSF.

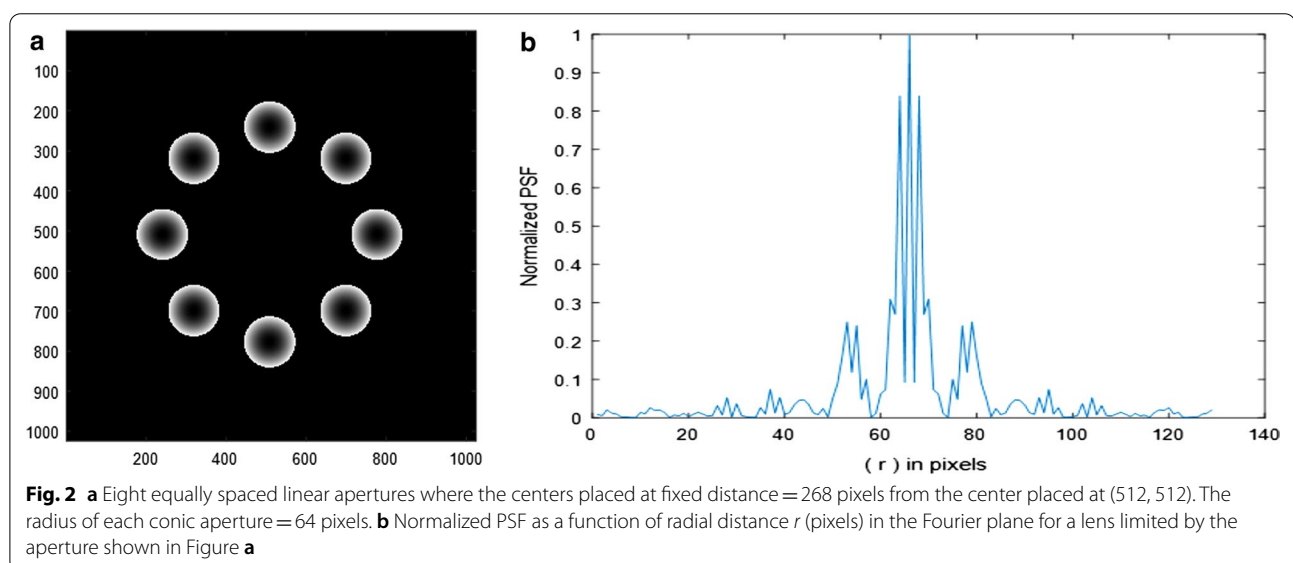
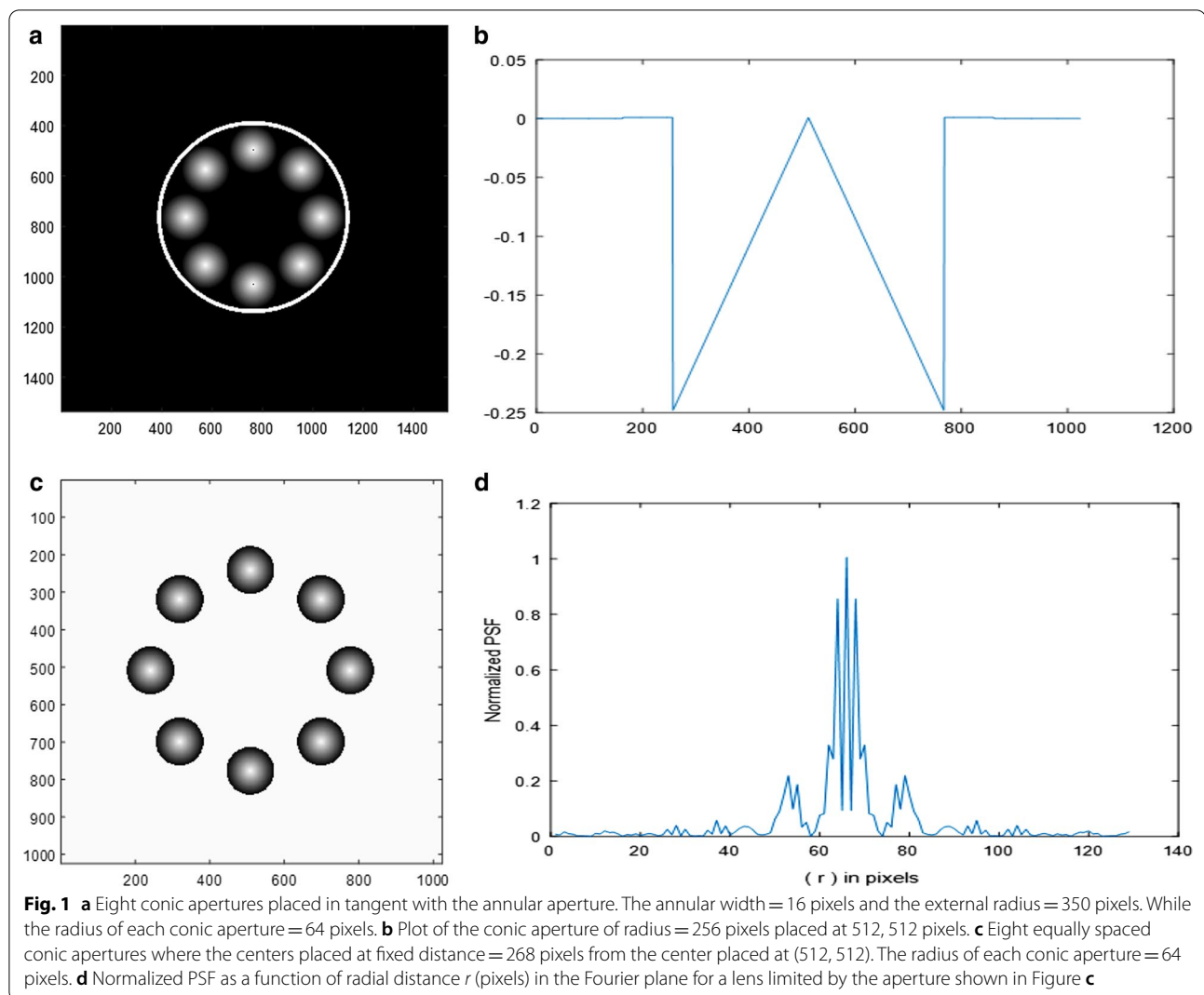
Similarly, the PSF is computed for the other eight equally spaced apertures of the linear and the quadratic distributions using the FFT technique.

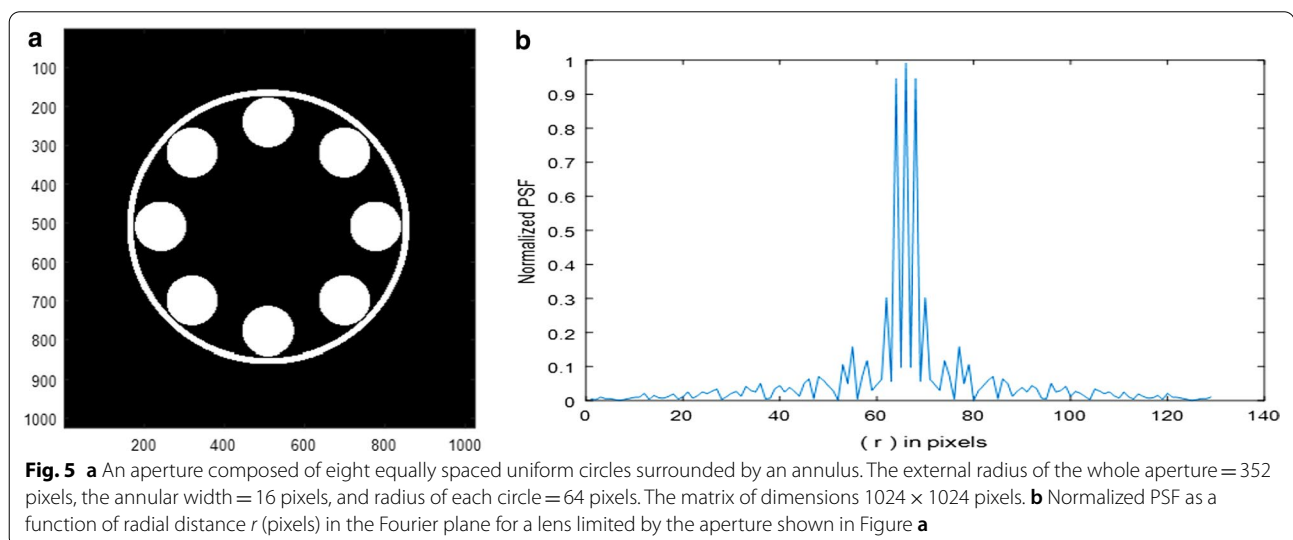
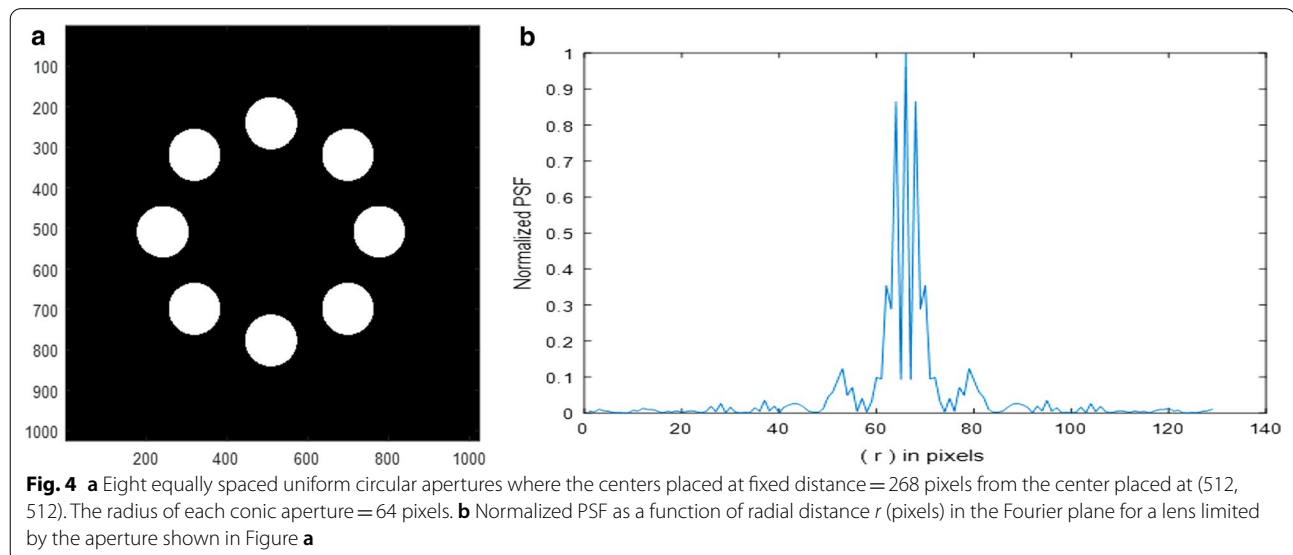
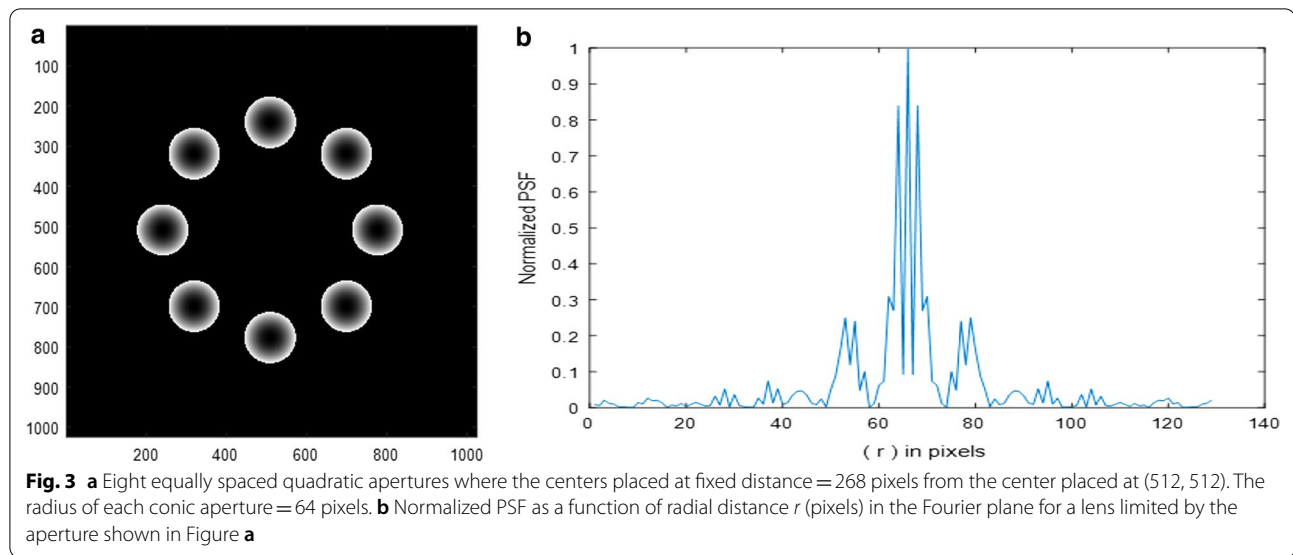
## 3 Results

Design of eight conic apertures placed in tangent with the annular aperture is shown in Fig. 1a. The annular width = 16 pixels and the external radius = 350 pixels. While the radius of each conic aperture = 64 pixels. A plot of the conic aperture of radius = 256 pixels placed at 512, 512 pixels is shown in Fig. 1b. Eight equally spaced conic apertures where the centers placed at fixed distance = 268 pixels from the center placed at (512, 512) are shown in Fig. 1c. The radius of each conic aperture = 64 pixels.

The PSF is computed using FFT for all apertures. The Normalized PSF as a function of radial distance  $r$  (pixels) in the Fourier plane for a lens limited by the aperture in Fig. 1c is shown in Fig. 1d. While for the same arrangement for the apertures described above is shown in Figs. 2a and 3a for the linear and quadratic distributions. The corresponding plots of normalized PSF are shown in Figs. 2b and 3b. Finally, eight equally spaced uniform circular apertures shown in Fig. 4a are shown for comparison. The corresponding normalized PSF plot is shown in Fig. 4b. The same arrangement surrounded by an annulus and its corresponding normalized PSF are shown in Fig. 5a, b. The normalized PSF showed similar shapes for the eight conic, linear, and quadratic apertures.

The autocorrelation images and their line plots at the center are computed using FFT techniques, for the conic, linear, quadratic, and uniform circular as shown in Fig. 6a–d.





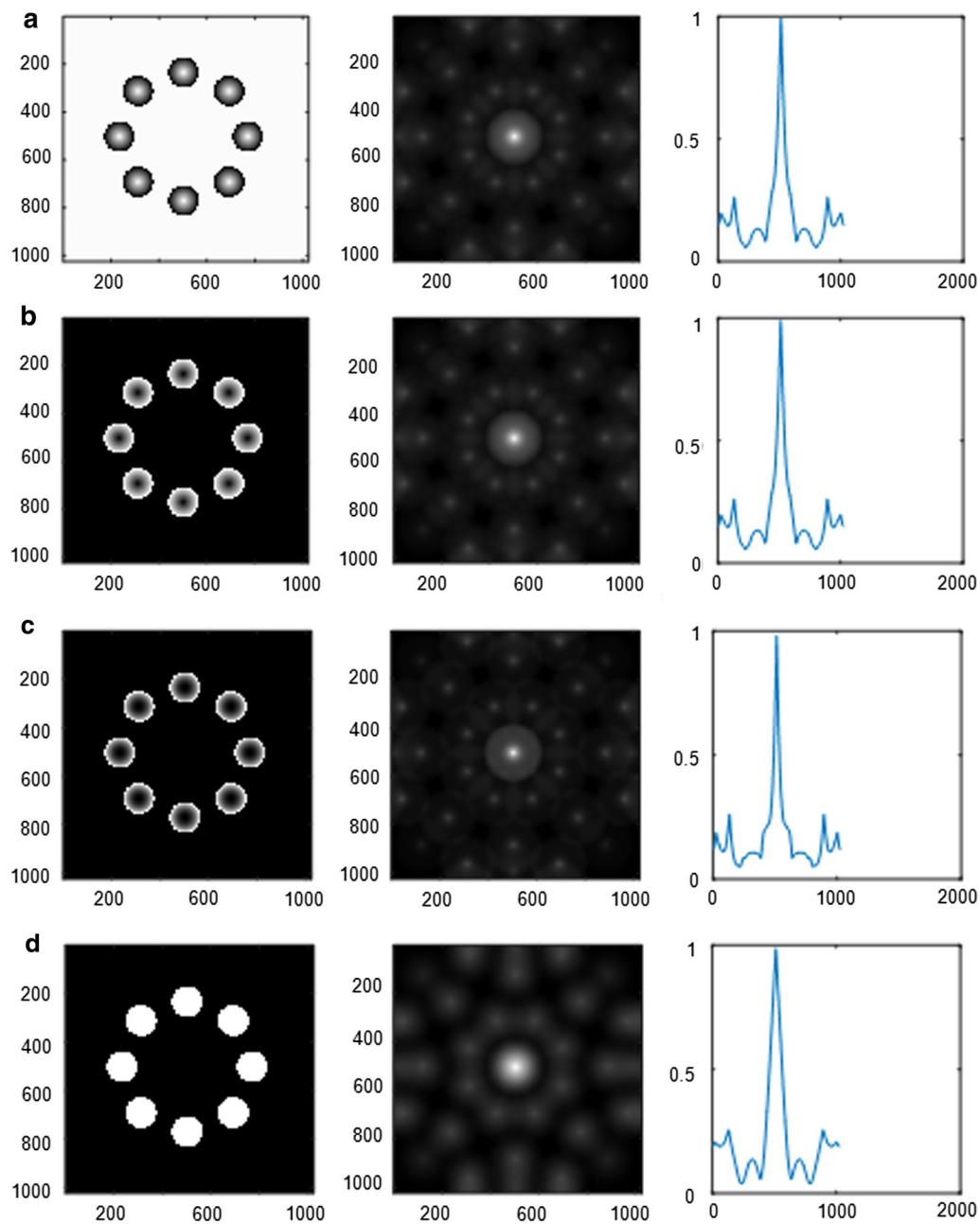


**Fig. 6** **a** Autocorrelation image and the plot for the conic aperture. **b** Autocorrelation image and the plot for the linear aperture. **c** Autocorrelation image and the plot for the Quadratic aperture. **d** Autocorrelation image and the plot for the uniform circular aperture

The line plot corresponding to the autocorrelation of the conic and the uniform circular models are plotted as shown in Fig. 7a, b.

Finally, speckle images formed using the above apertures combined with the same diffuser are computed and plotted as shown in the L.H.S. of Fig. 8a–c for conic, linear, and uniform circles, respectively. The reconstructed images of

apertures are obtained using the inverse FFT as shown in the R.H.S. of Fig. 8.

#### 4 Discussions

It is shown, referring to the plotted PSF corresponding to the apertures in Figs. 1, 2, 3, 4, and 5 a great similarity in the distribution, in the central peak. In addition, a noticeable difference is shown in the legs of the patterns for all

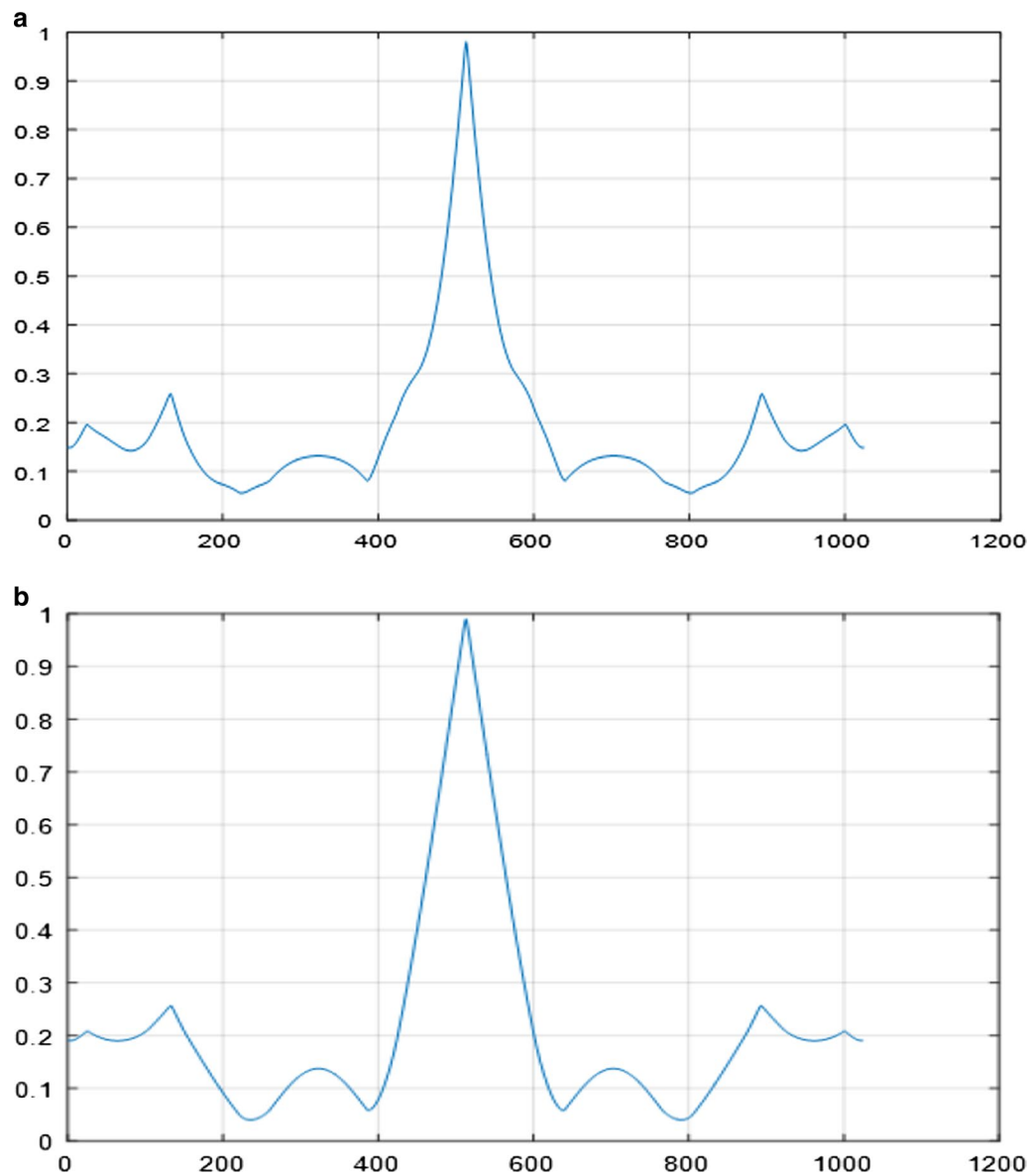


**Fig. 7** **a** Autocorrelation of conic model. **b** Autocorrelation of circular uniform model

the plots, while a remarkable difference is in Fig. 5b since the model is surrounded by annulus as expected. Consequently, the PSF distribution is mainly dependent upon the aperture distribution assuming monochromatic light for the illumination. It is shown different irregular shape for the legs of the diffraction pattern.

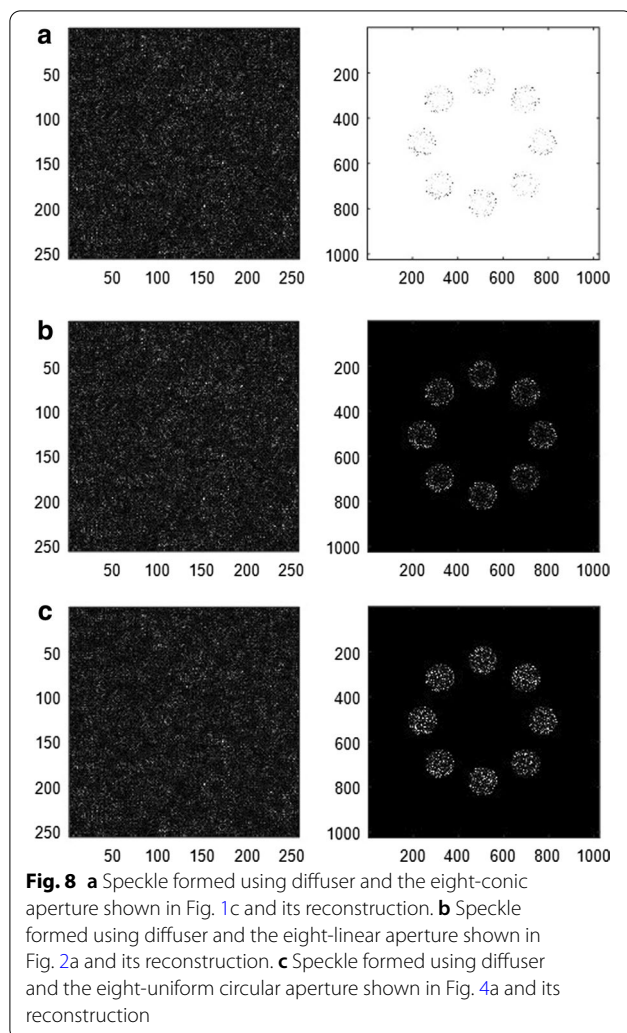
Referring to Fig. 7a, b corresponding to the autocorrelation plots, it is shown smooth pattern for the circular arrangement as compared with the deformation and shrinking appeared in the central peak in case of conic model. In addition, the total width corresponding to the autocorrelation is two times the aperture diameter as expected.

The reconstructed images of apertures shown in Fig. 8 are affected by a noise originated from the diffuser. The reconstructed images may be improved using Wiener filtering allowing to reduce the produced noise from the diffuser.

## 5 Conclusions

We have manufactured apertures in the form of equally spaced conic, linear, and quadratic circles. The normalized PSF computed for all apertures have nearly the same shape. In addition, the autocorrelation corresponding to





the apertures is computed and plotted. Finally, speckle imaging using diffuser limited by the manufactured apertures are computed and plotted. The reconstructed apertures are obtained from the speckle images which can be improved by filtering techniques.

#### Abbreviations

PSF: Point spread function; FFT: Fast Fourier transform; DFT: Discrete Fourier transform; LSCI: Laser speckle contrast images.

#### Acknowledgements

Not applicable.

#### Authors' contributions

The author read and approved the final manuscript.

#### Funding

Not applicable.

#### Availability of data and materials

Not applicable.

## Declarations

#### Ethics approval and consent to participate

Not applicable.

#### Consent for publication

Not applicable.

#### Competing interests

The author declares that he has no competing interests.

Received: 21 December 2021 Accepted: 8 March 2022

Published online: 18 March 2022

## References

- Goodman JW (1976) Some fundamental properties of speckle. *J Opt Soc Am* 66(11):1145–1150
- Francon M (ed) (1979) *Laser speckle and applications in optics*, 1st edn. Elsevier. ISBN: 978-0-323-16072-8
- Dainty C (ed) (1984) *Laser speckle and related phenomena*, 2nd edn. Springer-Verlag. ISBN 978-0-387-13169-6
- Goodman JW (1975) Statistical properties of laser speckle patterns. In: Dainty JC (ed) *Laser speckle and related phenomena, topics in applied physics*, vol 9. Springer, Berlin, pp 9–75
- Fercher F, Briers JD (1981) Flow visualization by means of single-exposure speckle photography. *Opt Commun* 37(5):326–330
- Barrera JF, Henao R et al (2006) Multiple image encryption using an aperture-modulated optical system. *Opt Commun* 261(1):29–33
- Salazar A, Telbadi M et al (2003) Experimental study of volume speckle in four-wave mixing arrangement. *Opt Commun* 221:249–256
- Sheppard CJR (2012) Nonparaxial, three-dimensional and fractal speckle. In: *Proceedings of SPIE 8413, Speckle 2012: V international conference on speckle metrology*, p 841302. <https://doi.org/10.1117/12.977790>
- Yuan S, Devor A et al (2005) Determination of optimal exposure time for imaging of blood flow changes with laser speckle contrast imaging. *Appl Opt* 44:1823
- Richards LM, Kazmi SMS et al (2013) Low-cost laser speckle contrast imaging of blood flow using a webcam. *Biomed Opt Express* 4:2269
- Davis MA, Kazmi SMS, Dunn AK (2014) Imaging depth and multiple scattering in laser speckle contrast imaging. *J Biomed Opt* 18:086001
- Kazmi SMS, Richards LM et al (2015) Expanding applications, accuracy, and interpretation of laser speckle contrast imaging of cerebral blood flow. *J Cereb Blood Flow Metab* 35:1076–1084
- Davis MA, Gagnon L et al (2016) Sensitivity of laser speckle contrast imaging to flow perturbations in the cortex. *Biomed Opt Express* 7:759
- Parthasarathy AB, Weber EL et al (2010) Laser speckle contrast imaging of cerebral blood flow in humans during neurosurgery: a pilot clinical study. *J Biomed Opt* 15:066030
- Ponticorvo A, Dunn AK (2010) How to build a laser speckle contrast imaging (LSCI) system to monitor blood flow. *J Vis Exp* 45:2004. <https://doi.org/10.3791/2004>
- Boas DA, Dunn AK (2010) Laser speckle contrast imaging in biomedical optics. *J Biomed Opt* 15:011109
- Briers D, Duncan D (2013) Laser speckle contrast imaging: theoretical and practical limitations. *J Biomed Opt* 18(6):66018. <https://doi.org/10.1117/1.JBO.18.6.066018>
- Briers JD, Webster S (1996) Laser speckle contrast analysis (LASCA): a non-scanning, full-field technique for monitoring capillary blood flow. *J Biomed Opt* 1(2):174–179
- Thompson O, Andrews M, Hirst E (2011) Correction for spatial averaging in laser speckle contrast analysis. *Biomed Opt Express* 2(4):1021–1029
- Hamed AM (2021) Contrast of laser speckle images using some modulated apertures. *J Phys Pram* 95:122. <https://doi.org/10.1007/s12043-021-02151-8>
- Hamed AM (2009) Numerical speckle images formed by diffusers using modulated conical and linear apertures. *J Mod Opt* 56(10):1174–1181. <https://doi.org/10.1080/09500340902985379>

22. Hamed AM (2017) Improvement of point spread function (PSF) using linear-quadratic aperture. *Optik* 131:838–849. <https://doi.org/10.1006/j.ijleo.2016.11.211>
23. Hamed AM (2021) Speckle imaging of annular Hermite Gaussian laser beam. *J Phys Pram* 95:202. <https://doi.org/10.1007/s12043-021-02231-9>
24. Taya Sofyan A, Hussein Aya J et al (2021) Dispersion curves of a slab waveguide with a nonlinear covering medium and an exponential graded-index thin film. *J Opt Soc Am* 38(11):3237–3243
25. Hussein Aya J, Nassar Zaher M, Taya Sofyan A (2021) Dispersion properties of slab waveguides with a linear graded-index film and a nonlinear substrate. *Microsyst Technol* 27(7):2589–2594
26. Hussein Aya J, Taya Sofyan A (2021) Universal dispersion curves of a planar waveguide with an exponential graded index guiding layer and a nonlinear cladding. *Results Phys* 20:6, Article 103734
27. Upadhyay A, Singh S et al (2021) An ultra-high birefringent and nonlinear decahedron photonic crystal fiber employing molybdenum disulphide ( $\text{MoS}_2$ ): a numerical analysis. *Mater Sci Eng B* 270:115236

## Publisher's Note

Springer Nature remains neutral with regard to jurisdictional claims in published maps and institutional affiliations.

**Submit your manuscript to a SpringerOpen<sup>®</sup> journal and benefit from:**

- Convenient online submission
- Rigorous peer review
- Open access: articles freely available online
- High visibility within the field
- Retaining the copyright to your article

---

Submit your next manuscript at ► [springeropen.com](https://www.springeropen.com)

---